Size-Selective Synthesis and Stabilization of Gold Organosol in C_nTAC: Enhanced Molecular Fluorescence from Gold-Bound Fluorophores

Snigdhamayee Praharaj, Sujit Kumar Ghosh, Sudip Nath, Subrata Kundu, Sudipa Panigrahi, Soumen Basu, and Tarasankar Pal*

Department of Chemistry, Indian Institute of Technology, Kharagpur 721302, India

Received: March 4, 2005; In Final Form: May 22, 2005

Gold nanoparticles of variable sizes have been synthesized in toluene employing two-phase (water−toluene) extraction of $AuCl_4^-$ followed by its reduction with sodium borohydride in the presence of a series of cationic surfactants of a homologous series having the general formula C_nTAC. The solubility features of the gold particles in the organic solvent have been accounted qualitatively by calculating the van der Waals interaction potential between the particles. The effect of thermal energy and medium dielectric constant on the stability of metal particles has been studied by measuring the surface plasmon resonance. The stabilization of surfactant-mediated gold particles as hydrosol or organosol has been elucidated by considering the double-layer interaction as a function of the dielectric constant of the solvent medium. The influence of the counterion of the phase transfer reagent and stabilizing ligand on the photochemical stability of the gold colloids has been investigated. The fluorescence probe 1-methylaminopyrene (MAP) was considered for the surface functionalization of the gold particles, and it has been found that there is an enhancement of molecular fluorescence from the gold−probe assembly.

Introduction

During the last few decades, the emerging field of nanosized transition metal particles has stimulated much research interest due to their unique physical and chemical properties, which are quite different from those of the corresponding bulk materials.[1−5] Tremendous effort has been made to optimize their uses as catalysts, ferrofluids, and sensors as well as their potential applications in a new generation of optical, electronic, and magnetic devices.[2−5] Materials in the nanometer size regime exhibit size- or shape-dependent optical properties as a consequence of the quantum size effect and high surface-to-volume ratio of the particles.[6,7] Hence, a burst of current research activities has been devoted to the size- and shape-selective synthesis and characterization of noble metal nanoparticles.

Among all metal nanoparticles, copper, silver, and gold are the most interesting due to their characteristic optical properties arising due to strong interactions with visible light through resonant excitations of the collective oscillations of the conduction electrons within the particles.[8] The resonant frequency of metallic nanoparticles is known to be dependent on size, shape, interparticle coupling, material properties, and surrounding environment.[6a,9−12] At a fundamental level, the optical absorption spectra provide information on the electronic structure of small metallic particles. Again, engineering of nanocluster surfaces with electroactive or photoactive molecules can provide three-dimensional molecular arrangements around the nanoparticles.[13−15] Since fluorescence spectroscopy is a very sensitive technique, fluorophore-bound gold nanoparticles have become useful probes for biomolecular labeling, complementary sensing via fluorescence spectroscopy, and electron microscopy.

A few synthetic routes have been reported in the literature for the size-selective synthesis of metal colloids in organic solvents. Klabunde et al.[16] reported the digestive ripening method for converting a polydisperse colloidal suspension to a highly monodisperse one using C_8SH to $C_{16}SH$ chain length thiols, and in this procedure, the particle size increases from 4.5 to 5.5 nm with an increase in the thiol chain length. Zhang and colleagues[17] described the preparation of shell−core nanostructured composites of *trans*-4-(mercaptoheptoxy)stilbene capped as a monolayer on colloidal gold clusters of diameters ranging from 1.4 to 5.2 nm. Again, methodologies pertaining to the synthesis of novel gold nanoparticles bearing cationic single-chain, double-chain, and cholesterol-based amphiphilic units with average diameters of 5.9, 2.9, and 2.04 nm have also been reported.[18] In that case, the average size of the resultant nanoparticles was controlled by the relative bulkiness of the capping agent.

In this article, we have reported the size-selective synthesis of gold nanoparticles with average diameters from 9 to 15 nm in toluene using cationic surfactants of variable chain lengths bearing the general formula C_nTAC as the stabilizing ligand. The particles have been characterized by UV−visible spectroscopy and transmission electron microscopic (TEM) studies. The solubility features of the gold particles in toluene have been accounted qualitatively by calculating the van der Waals interaction potential between the spherical gold cores of the nanoparticles stabilized by the surfactants of variable chain lengths. The effect of temperature on the surface plasmon resonance of the organosol has also been studied. The stability of the surfactant-stabilized gold nanoparticles in aqueous and organic solvents has been elucidated by considering the double-layer interaction as a function of the medium dielectric constant. The importance of the counterion of the phase transfer reagent and stabilizing ligand on the photochemical stability of the gold colloids has been discussed. Finally, a fluoroprobe, 1-methylaminopyrene, was employed for the surface modification of the

* Corresponding author. E-mail: tpal@chem.iitkgp.ernet.in.

10.1021/jp051132n CCC: $30.25
Published on Web 06/21/2005

gold particles, and it has been found that there is an enhancement of molecular fluorescence from the gold−probe assembly.

Experimental Section

Reagents and Instruments. All the reagents used were of AR grade. Chloroauric acid ($HAuCl_4 \cdot 3H_2O$), cetyltrimethylammonium bromide (CTAB), and sodium borohydride were purchased from Aldrich. Cetyltrimethylammonium chloride (C_{16}TAC) and other cationic surfactants of different chain lengths (C_{10}, C_{12}, C_{14}, and C_{18}) of the homologous series were obtained from Aldrich and were used without further purification. Phase transfer agents, namely, tetraethylammonium chloride (TEAC) and tetraethylammonium bromide (TEAB), were used as received from Aldrich. Solvents, namely, toluene and tetrahydrofuran (THF), were purchased from Merck and were dried before use. The fluorescent probe 1-methylaminopyrene (MAP) was purchased from Aldrich and was used as received.

The absorption spectrum of each solution was recorded in a Spectrascan UV 2600 digital spectrophotometer (Chemito, India) in a 1 cm well-stoppered quartz cuvette, and the solvent background was subtracted each time. The emission spectra were measured in a Spex Fluorolog-3 (model no. FL3-11) fluorescence spectrophotometer. All the emission and excitation spectra were corrected for detector sensitivity and lamp intensity fluctuations with respect to wavelength. An excitation wavelength of 328 nm and a slit width of $^2/_2$ nm were used to record the spectra. Photoirradiations were carried out with a photoreactor fitted with germicidal lamps of UVC G8 T5 (Sankyo Denki, Japan) with a wavelength of 365 nm and a UV-light flux of ∼850 lux (1 lumen flux of photon per cm^2 per s). Photochemical reactions were carried out in the quartz cuvette. The cell was kept in an upright position and 3 cm apart from the light source. Electron micrographs of the metal colloids were measured with a Hitachi H-9000NAR transmission electron microscope, operating at 200 kV. The samples were prepared by mounting a drop of the solution on a carbon-coated copper grid and allowing it to dry under vacuum.

Synthesis of Gold Organosol Stabilized by Surfactants of Variable Chain Lengths. The synthesis of cationic-surfactant-stabilized gold nanoparticles was carried out in a two-step procedure. In a typical preparation, $AuCl_4^-$ was first transferred from an aqueous solution to toluene using tetraethylammonium chloride as the phase transfer reagent and was, then, reduced with sodium borohydride in the presence of a series of cationic surfactants, C_nTAC, as the stabilizing agent. Upon the addition of the reducing agent, the toluenic solution changed color from light yellow to the characteristic color of gold colloids within a few minutes.

The preparation technique is as follows. To an aqueous solution of $HAuCl_4$ (100 mL, 0.5 mM), 20 mg of TEAC was added and toluene (100 mL) was introduced above the aqueous layer. Upon shaking, $AuCl_4^-$ ions were transferred from the aqueous phase to the organic layer. The organic phase was separated and divided into five equal portions. Five different surfactants bearing C_nTAC ($n = 10$, 12, 14, 16, or 18) moieties were added and mixed well so that the final concentration of C_nTAC in all of the sets was maintained at 5 mM. Finally, 2 mg of sodium borohydride was introduced into each solution and all the reaction mixtures were shaken vigorously. During shaking, at first, the yellow color due to $AuCl_4^-$ disappeared and the solution became colorless within a few minutes. The solution turned into the characteristic color of gold colloids upon further shaking. The method is reproducible, and the final concentrations of gold in this experiment were 0.5 mM. The stability of the metallic particles is discussed in detail a later section. The metallic dispersion in toluene can be dried under vacuum and redispersed in toluene and other common organic solvents without any sign of aggregation or precipitation of the particles.

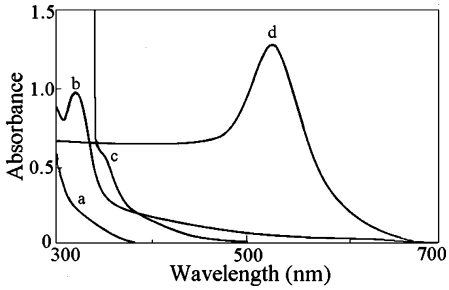

Figure 1. Absorption spectra of a toluenic dispersion of (a) C_{18}TAC, (b) $[TEA]^+[AuCl_4]^-$, (c) $[C_{18}TA]^+[AuCl_4]^-$, and (d) C_{18}TAC capped Au nanoparticles. Conditions: $[HAuCl_4] = 0.5$ mM and $[C_{18}TAC] = 5$ mM. The volume of the solution was 20 mL with toluene; spectra were taken at an optical path of 1 cm.

Making the Gold−Probe Assembly. The metallic particles prepared by the above method (stabilized by C_{18}TAC) were evaporated to ∼2 mL in a rotary evaporator, resulting in a gold concentration of 5.0 mM. This highly concentrated gold suspension in toluene was diluted with THF to have a concentration of 0.5 mM. In a typical set, a known amount of MAP (1.0 μM) in THF was added to the gold suspension (10 μM) in THF (THF solution thus contained ∼1% toluene) so that the final volume of the solution was maintained at 3 mL in a 1 cm well-stoppered quartz cuvette. The solution was allowed to stand for ∼6 h to complete the surface complexation process, and the emission spectrum was measured in the spectrofluorimeter.

Results and Discussion

Evolution of Gold Nanoparticles in Toluene. Figure 1 shows the absorption spectral features for the evolution of gold nanoparticles in toluene. The toluenic dispersion of C_{18}TAC shows no characteristic absorption maximum in the range 300−700 nm (trace a). Conversely, the $[TEA]^+[AuCl_4]^-$ ion pair in toluene exhibits an absorption maximum at 323 nm (trace b), relating to the metal-to-ligand charge transfer (MLCT) band of $AuCl_4^-$ complexes.[19] Addition of C_{18}TAC to the toluenic solution of Au(III) causes the 323 nm absorption band to vanish due to $AuCl_4^-$ complexes, and a new absorption band appears with a shoulder at ∼355 nm (trace c) that can be ascribed to the formation of the ion pair $[C_{18}TA]^+[AuCl_4]^-$ ($[C_{18}TA]^+$ = octadecyltrimethylammonium ion). Upon the addition of $NaBH_4$ into the reaction mixture, the yellow color of the solution gradually disappears, and after a certain time, the solution becomes completely colorless, indicating the formation of AuO_2^- species in the alkaline condition.[20] Upon further shaking, the appearance of the pinkish tinge within the solution indicates the onset of the evolution of gold particles. The color of the solution gradually changes from light pink to red to wine red upon completion of the reaction. Absorption measurement of this resulting solution shows a new absorption band with a maximum at 525 nm (trace d), which corresponds to a typical plasmon band of gold nanoparticles. Similar trends in the absorption spectral features are also observed during the evolution of gold particles in the presence of other cationic surfactants.

Characterization of the Gold Particles. The surface plasmon absorption of gold nanoparticles in the presence of different cationic surfactants is shown in Figure 2. The absorption maxima

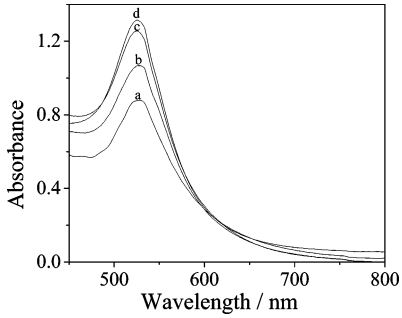

Figure 2. Surface plasmon absorption band of gold nanoparticles (0.5 mM) stabilized by (a) C_{12}TAC, (b) C_{14}TAC, (c) C_{16}TAC, and (d) C_{18}TAC in toluene.

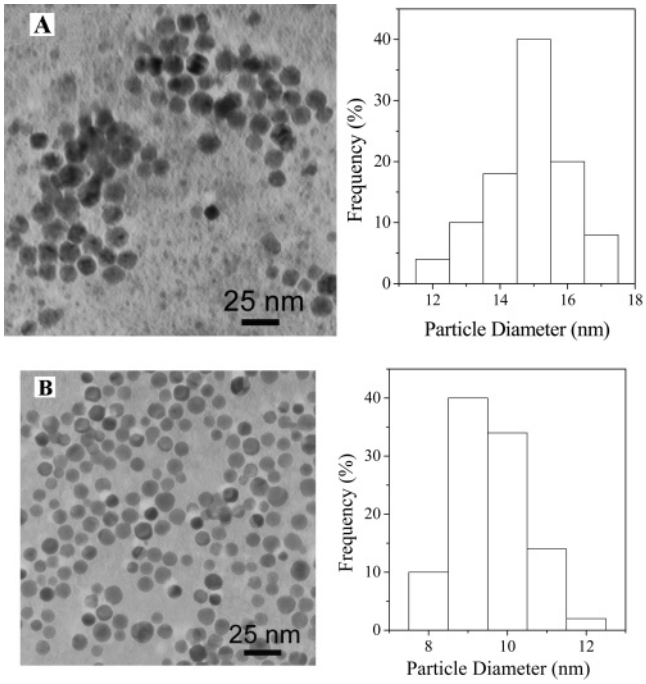

Figure 3. TEM images and the corresponding diameter histogram of gold colloids stabilized by (A) C_{12}TAC and (B) C_{18}TAC.

in toluene appear at 526 nm for C_{12}TAC-stabilized gold particles, 525.5 nm for C_{14}TAC- and C_{16}TAC-stabilized gold particles, and 525 nm for C_{18}TAC-stabilized gold particles. In the case of C_{10}TAC, the particles leave a bluish precipitate immediately after the preparation. Parts A and B of Figure 3 show the representative TEM images for the gold colloids and the corresponding diameter histogram for C_{12}TAC- and C_{18}TAC-stabilized particles, respectively. It is seen that the chain length of cationic surfactants has an influence on the particle size but not on the morphology of the finally formed stable colloids. The particles are spherical or nearly spherical in all cases, and the average particle sizes have been measured as 15 $\pm$ 1.4, 13 $\pm$ 0.9, 11 $\pm$ 0.6, and 9 $\pm$ 0.4 nm for C_{12}, C_{14}, C_{16}, and C_{18}TAC, respectively. The average particle size increases from 9 to 15 nm with decreasing chain length. The trend in the development of particle size is in contrast to the earlier observation of the Sorensen and Klabunde group.[16] They observed that the average particle size increased from 4.5 to 5.5 nm as the digestive ripening ligand was changed from C_8-SH to C_{16}SH and attributed this phenomenon to the fact that the lengthier ligands should prefer less curved surfaces favoring larger sized particles.

As mentioned above, the particle size varies with the variation in the surfactant chain length in toluene. Due to the increase in chain length of the surfactant, the particle size decreases (i.e., no. of particles increases) and the intensity of absorption increases for a particular concentration of Au(III) ion. According to the Mie theory, the molar absorption coefficient depends on particle volume in a linear fashion.[21] Table 1 emerges the fact that the concentration of the particles decreases as the size increases. A plot of molar absorption coefficient (k') versus particle volume leads to a straight line (Figure 4) which shows that the molar absorption coefficient varies linearly with particle volume.

Recently, it has been reported from our laboratory[22] that the chain length of cationic surfactants, C_nTAC ($n = 10-18$), has a profound influence on the evolution of gold nanoparticle morphology and also on their different states of aggregation in aqueous surfactant solution. This has been ascribed to the variation in concentration of the micelles and the micellar structures in aqueous solution with the chain length of the surfactants.

The chain length dependence of surfactants on the particle size could be explained in terms of the dynamic formation mechanism[23,24] in an ensemble of metal nanoparticles. It is now well-known that the final size of metallic nanoparticles in solution depends on many parameters, such as the solute concentration, redox potential of the reduction reaction, nature and concentration of the stabilizer, viscosity and surface tension of the solvent, and temperature.[6b,25-27] At the initial stages, there is rapid formation of embryonic particles. The atoms are, then, aggregated as fast as the atoms are supplied. This initial rapid aggregation continues until the atoms in close vicinity are depleted almost completely. As a result, embryonic nanoparticles are formed in a region void of the atoms. However, supply of atoms from the outside to the embryos through diffusion causes the particle to grow slowly even after the rapid growth process ceases. The slow growth is terminated due to the binding of the particle surface with the surfactant molecules, which diffuse through the solution toward the particle surface.[28] With the increase in the chain length of the surfactants, the diffusion of gold atoms/ions to the growing particles is hindered in succession and the particle growth becomes slower in competition with termination of the growth due to surfactant binding on the particle surface. As a result, with an increase in the chain length of the surfactant, the particle size decreases. Since organic solvents usually have lower dielectric constants than that of water, the degree of dissociation of metal complexes becomes lower and ligand-to-metal charge transfer decay is slower than in water.[29] This behavior affects the formation of particles through the reduction of metal ions, and therefore, the surfactant chain lengths cannot induce a large variation in the particle morphology likewise in the aqueous phase. It is now well established that the optical properties of gold colloids are highly dependent on the particle size and interparticle separation.[8,9,22] With a decrease in the chain length of the surfactant, the particle size increases and the interparticle separation between the particles decreases. Both of these factors are responsible for yielding a little red shift with the decrease in the chain length of the surfactants.

Stability of Gold Colloids

Effect of Surfactant Chain Length. The stability of metallic nanoparticles in the solution phase is an important issue, since naked metal nanoparticles are unstable in organic solvents, and therefore, some form of stabilizer is required to prevent the particle aggregation. Encapsulation of the particle core with an

TABLE 1: Correlation between the Molar Absorption Coefficient and the Particle Volume

chain length	C_{18}TAC	C_{16}TAC	C_{14}TAC	C_{12}TAC
particle size	9	11	13	15
concentration of the particles	2.2×10^{-8} M	1.2×10^{-8} M	7.4×10^{-8} M	4.8×10^{-8} M
aggregation no.	22 530	41 134	67 898	104 304
absorbance	1.32	1.25	1.07	0.87
volume of the particles	381.9	697.19	1150.81	1767.86
k'	0.59×10^8	1.04×10^8	1.49×10^8	1.77×10^8

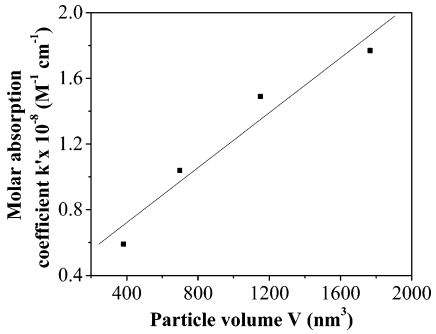

Figure 4. Plot of molar absorption coefficient vs particle volume of gold nanoparticles stabilized by different chain length surfactants.

TABLE 2: Correlation between the van der Waals Attraction Potential and the Particle Stability of Gold Nanoparticles Stabilized by Surfactants of Variable Chain Lengths

system	particle size (nm)	surfactant chain length (nm)	$V(D)$ $\langle k_BT \rangle$[a]	stability
Au−C_{10}TAC		1.80		aggregated instantaneously
Au−C_{12}TAC	15 ± 1.4	2.08	−1.7	2−3 h
Au−C_{14}TAC	13 ± 0.9	2.31	0.7	≤7 days
Au−C_{16}TAC	11 ± 0.6	2.57	1.6	20 days
Au−C_{18}TAC	9 ± 0.4	2.84	6.9	>2 months

[a] Here, k_B denotes the Boltzmann constant and T is the temperature (=300 K).

appropriate shell material offers a means of protection from the surrounding environment. Independent manipulation of the core and shell composition provides a way to engineer optical functionality of the particles. These types of nanoparticles have been referred to as the "core−shell" particles, consisting of metal cores with a dielectric shell.[30] Although the alkyl chain lengths of the surfactants are unable to induce a large variation in the particle morphology, it is very interesting to note the stability of the gold particles in surfactants of varying chain lengths. The chain lengths of the surfactants have a profound influence on the stability of the gold particles. The Au−C_{10}TAC colloid settles down instantaneously just after the preparation to the bottom of the round-bottom flask, leaving a clear, colorless supernatant. The Au−C_{12}TAC colloid is precipitated after 2−3 h of their preparation. The Au−C_{10}TAC and Au−C_{12}TAC assemblies look alike at the bottom of the flask, but the supernatant still remains slightly purple in the case of Au−C_{12}-TAC. There is no such aggregation or precipitation of the particles in the cases of Au−C_{14}TAC and Au−C_{16}TAC colloids in a week or so, while Au−C_{18}TAC particles remain as such even after a couple of months.

The solubility features of the gold particles could be accounted qualitatively by calculating the interaction potential which is approximately given by the dispersional attractions between the spherical gold cores of the nanoparticles. The van der Waals attraction potential between two solid spheres of radii R_A and R_B is given by[31]

$$V(D) = -\frac{A}{12}\left[\frac{R_r}{D[1 + D/2(R_A + R_B)]} + \frac{1}{1 + D/R_r + D^2/4R_AR_B} + 2\ln\left(\frac{1 + D/2(R_A + R_B)}{R_r[1 + D/R_r + D^2/4R_AR_B]}\right)\right] \quad (1)$$

where A is the Hamaker constant which is equal to 1.95 eV for gold, D is the distance of closest approach between two adjacent spheres, and R_r is the reduced radius given by $2R_AR_B/(R_A + R_B)$. For a fixed set of gold nanoparticles, inducing tight size approximation, $R_A = R_B = R$ and the above equation simplifies to

$$V(D) = -\frac{A}{12}\left[\frac{R_r}{D[1 + D/4R]} + \frac{1}{1 + D/R_r + D^2/4R^2} + 2\ln\left(\frac{1 + D/4R}{R_r[1 + D/R_r + D^2/4R^2]}\right)\right] \quad (2)$$

The attraction energies as a function of the particle size, distance of nearest surfaces of adjacent spheres, and the stability of the gold particles are shown in Table 2. We have assumed that the two spheres are separated by the chain length of the surfactants attached to the gold particles at the moment of closest approach between the particles. From Table 2, it is seen that the attraction potential has a negative value in the case of Au−C_{12}TAC but it is positive for gold particles stabilized by surfactants containing longer chain lengths.

The gold nanocores being negatively charged (due to the adsorption of negatively charged Cl^-), C_nTA^+ ions are bound to the gold surface via the headgroups and are connected to the outer layer through hydrophobic interactions.[32] Thus, the steric stabilization arising due to the attachment of the surfactants on metal particles causes a screening of the unbalanced attractive van der Waals force.[33] Due to the smaller chain lengths of C_{10}-TAC and C_{12}TAC, these surfactants cannot provide enough hydrophobicity, enabling them to overcome van der Waals attractive forces, and this leads to aggregation of the particles. The Au−C_{12}TAC colloid is a kind of mixture of both the precipitated and suspended particles, perhaps in equilibrium with each other. The precipitate is due to the aggregation of the particles, which settle down at the bottom of the round-bottom flask due to gravitational forces, and the separated particles still remain suspended in solution. On the other hand, longer chain lengths of the surfactants are compatible enough to render hydrophobicity to the evolved gold particles and favor the particles to remain suspended in solution.

Effect of Temperature. During the evolution of metallic particles in the nanometer size regime in solution, the particles are susceptible to coalescence due to van der Waals attraction between the particles. Even in the absence of van der Waals

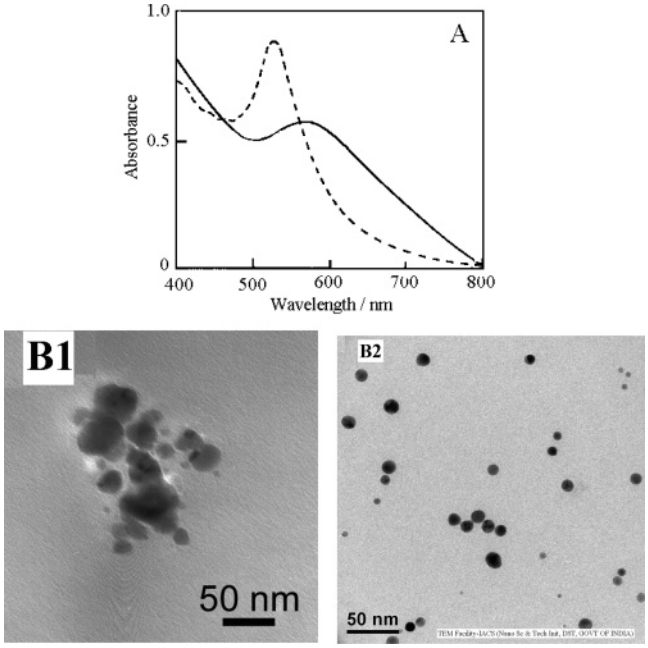

Figure 5. (A) Surface plasmon absorption band of Au−C_{10}TAC in toluene (—) before and (− − −) after heating. (B1 and B2) TEM images of the corresponding gold particles.

interaction, Brownian encounters are frequent enough to cause aggregation of the nanoparticles within a few seconds.[34] In the present experiment, during the evolution of gold nanoparticles in toluene in the presence of C_{10}TAC, metallic particles are precipitated instantaneously at the bottom of the round-bottom flask with a clear, colorless supernatant. Heating the reaction mixture in a water bath ruptures the aggregation and renders the particles to remain suspended in solution. Visual inspection shows the redispersion of particles with red coloration. In colloid chemistry, it is conventional to take 5−10 k_BT as the necessary barrier for the reasonable colloid stability.[35] Heating the reaction mixture promotes the particles to be dispersed, providing thermal energy enabling them to overcome the barriers, leading to coalescence. These results suggest that, at high temperatures, $T \geq 60$ °C, the colloids become soluble in toluene, but at room temperature, their tendency to form aggregates increases with decreasing alkyl chain length of the surfactants. When the metal colloid is again cooled to room temperature, the particles become aggregated and this phenomenon goes on reversibly up to four cycles with alternative heating and cooling of the solution.

Figure 5A exhibits the absorption spectral features before and after heating of the Au−C_{10}TAC colloids. Before heating, the UV−vis spectra of the vigorously shaken colloid shows a broad band with a maximum at ∼570 nm (solid line), corresponding to the blue color of the colloids. Upon heating the gold colloids, an absorption band develops with a maximum of ∼525 nm (dotted line) that can be attributed to the characteristic surface plasmon resonance of the dispersed gold nanoparticles. This arises from the collective oscillation of the free conduction band electrons that are induced by the incident electromagnetic radiation. It is now well documented in literature that the assembly of nanoparticles in various states of aggregation influences the plasmon resonance.[22,36−39] The broad band observed for Au−C_{10}TAC (Figure 5, solid line) illustrates that the particles are forming aggregates in solution. Due to interparticle coupling effects, there is an increase in the dielectric constant of the particles (arising due to electromagnetic interaction between the particles), shifting the plasmon peak to lower energies.[21] The TEM image of the Au−C_{10}TAC colloids shows

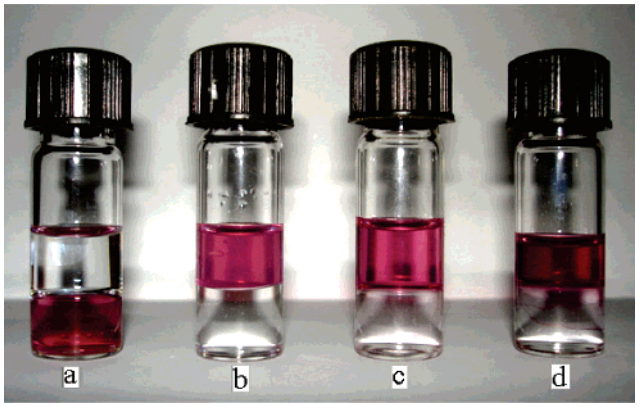

Figure 6. Original images of (a) C_{12}TAC-, (b) C_{14}TAC-, (c) C_{16}TAC-, and (d) C_{18}TAC-stabilized gold colloids. The photographs show the inherent tendency of Au−C_{14}TAC, Au−C_{16}TAC, and Au−C_{18}TAC particles to remain in the toluene layer while Au−C_{12}TAC particles are readily transferred to the aqueous phase.

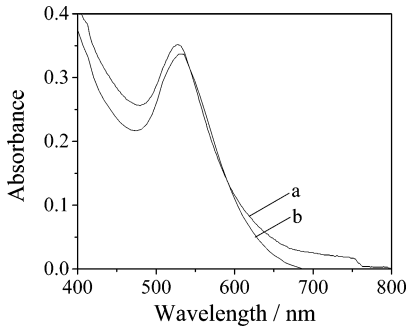

Figure 7. Surface plasmon band of Au−C_{12}TAC in (a) toluene and (b) water.

that the aggregated particles (Figure 5B1) become monodispersed upon heating (Figure 5B2).

Effect of Medium Dielectric Constant on the Dispersion of Gold Colloids: Hydrosol versus Organosol. Previously, it has been mentioned that gold nanoparticles stabilized by surfactants containing longer chains (C_{14}, C_{16}, and C_{18}) remain stable in the toluene layer, while gold particles mediated with smaller chain lengths (C_{12}) get precipitated. Keeping this observation in mind, we intended to study the effect of an aqueous/organic medium on the stability of a metal colloid dispersion. To study the phenomenon, 2 mL of water was introduced in all of the sets, containing 2 mL of the gold organosol in toluene. Figure 6 clearly accounts for the fact that the C_{14}TAC-, C_{16}TAC-, and C_{18}TAC-stabilized gold nanoparticles remain in the toluene layer (above water) while gold particles stabilized by C_{12}TAC move to the aqueous layer without any sort of agglomeration. This organosol-to-hydrosol transformation takes place without the addition of phase transfer reagent, and the particles remain stable for months together. The exhibition of the surface plasmon band of Au−C_{12}TAC in both organic and aqueous phases (Figure 7) authenticates the fact. Although a shift in the absorption maximum is observed due to phase transfer of the colloidal particles, the observed shift could arise from the effect of the different refractive indices of the solvents during transfer.[34]

The stability of suspensions of solid particles in a liquid medium is ensured by the repulsion between the particles.[33] The interparticle repulsion can be induced by two ways: electrostatic stabilization and steric stabilization. The former is the main cause for the stabilization of particles in aqueous solution. In the case of gold particles prepared by Frens' citrate reduction

procedure, the citrate ions are adsorbed onto the surface of the gold particles and, as a result, the particle surface becomes negatively charged. The cations in solution, then, form an electrical double layer around the gold particles. The double-layer interaction between two colloidal particles of radius R is given approximately by[39,40]

$$V/k_BT = 2\pi\epsilon_r\epsilon_0 R\psi_0^2 \exp(-\kappa H) - AR/12H \qquad (3)$$

where H is the surface separation, A is the Hamaker constant, Ψ_0 is the electric potential at the particle surface, and κ is the diffuse layer screening parameter, which is given by

$$\kappa^2 = 2z^2F^2c_0/\epsilon_r\epsilon_0 RT \qquad (4)$$

where c_0 refers to the concentration of electrolyte (z:z) in the solvent, F ($=-AR/6H^2$) is the force determined from the deflection of the cantilever via Hooke's law, and $\epsilon_r\epsilon_0$ is the permittivity of the medium. The dielectric constant of toluene is 2.4, whereas water has a dielectric constant of 80.0 at 298 K. Thus, there is an ~6 times decrease in the diffuse layer screening parameter (κ) and consequent increase in the double-layer interaction potential employing water as the dispersion medium than the organic phase. In the aqueous phase, if the polarity of the solvent is high enough, it results in a Coulombic repulsion rendering sufficient stability to the particles. On the other hand, in organic media, the electrostatic effects might not normally be considered to be important and steric repulsion is the only way to stabilize the dispersions. The smaller chain lengths of the surfactants (C_{10}TAC and C_{12}TAC) make the nanoparticles less hydrophobic, and consequently, the metal particles prefer to remain as stable in the aqueous phase. In toluene, the smaller chain lengths of the surfactants are not compatible enough to render stability to the evolved gold particles through hydrophobic repulsion; that is, they cannot provide steric stability and hence the particles get precipitated.[41] All of the other surfactants (C_{14}TAC, C_{16}TAC, and C_{18}TAC) due to their longer chain lengths engender the nanoparticles to be hydrophobic and remain stable in the toluene layer depending on the chain length of the surfactants.

Effect of Bromide Counterion (CTAB instead CTAC): Discoloration of Colloidal Gold in UV Light. Following the elucidation of the Brust protocol for the synthesis and capping of gold colloids, George Thomas et al.[42] reported the preparation of tetraoctylammonium bromide (TOAB) capped gold nanoparticles. In an attempt to adopt a similar synthetic procedure, we employed cetyltrimethylammonium bromide (surfactant containing bromide as the counterion) as the stabilizing agent instead of cetyltrimethylammonium chloride. It is seen that the gold organosol synthesized in the presence of cetyltrimethylammonium bromide in toluene is decolorized within a few hours in the presence of UV light. When 2 mL of the gold sol was subjected to UV irradiation in a well-stoppered quartz cuvette, it was found that the color of the sol faded gradually from the bottom to the top of the cuvette and, finally, became colorless. Absorption measurement shows a gradual decrease in the optical density of the ~538 nm peak, assigned to the surface plasmon absorption of colloidal gold, and a concomitant increase in the intensity of a new peak at 289 nm (Figure 8). These results indicate that discoloration of the gold colloids occurs at the expense of the dissolution of the gold particles. Oxidation of the metal particles occurs within half an hour to yield a colorless solution. The appearance of a new peak at 289 nm can be ascribed to the metal-to-ligand charge transfer band (MLCT) in $AuBr_2^-$ complexes.[1d] On standing, the colorless

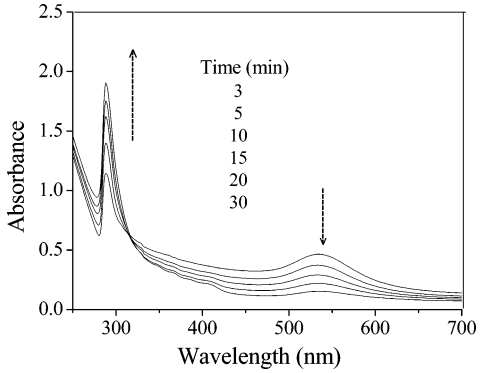

Figure 8. Absorption spectra of the successive dissolution of C_{16}TAB-stabilized gold nanoparticles and the simultaneous formation of $AuBr_2^-$ upon UV irradiation.

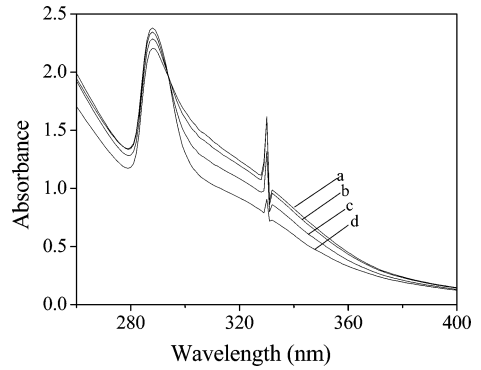

Figure 9. Absorption spectra of the successive dissociation of the $AuBr_4^-$ complex and the simultaneous formation of $AuBr_2^-$ upon (a) 0, (b) 10, (c) 20, and (d) 30 min of UV irradiation.

solution becomes slightly yellowish within a week or so. Absorbance measurement of this yellow solution shows a sharp absorption maximum at 330 nm in addition to 289 nm peaks, as shown in Figure 9. The appearance of the new peak at 330 nm indicates the formation of $AuBr_4^-$ complexes.[1d] UV illumination of the solution induced a bleaching of the absorption band at 330 nm, since $AuBr_4^-$ ions are photoreduced to regenerate $AuBr_2^-$ complexes (λ_{max} ~ 289 nm).[43,44] The photoinduced reversibility between $AuBr_4^-$ and $AuBr_2^-$ was reproduced for up to five cycles of operation without producing the metal atoms.

To understand the mechanism of photodecolorization, we repeated the Au sol preparation using TEAC and CTAC to obtain a system devoid of Br^-. Here, also, we observed photodecolorization. It was noticed that the absence of bromide ion retarded the decolorization process to a noticeable extent. Again, the process was repeated taking TOAB as the phase transfer reagent, whereas Au sol was stabilized by CTAB and CTAC for two separate sets. Similar decolorization was also observed in both cases. The photoproduced halide radicals have transient existence; however, they ($X^\bullet$) are generated continuously under UV irradiation.

The slower decolorization of Au sol in a system containing only $Cl^\bullet$ can be elucidated as follows. Chlorine has a higher electron affinity than bromine. Therefore, $Cl^\bullet$ and the solvated electrons recombine preferentially in the absence of any bromide ion. However, the presence of bromide ions in toluene in turn generates Cl^- along with $Br^\bullet$ which oxidizes gold. Thus, the slower decolorization process in the presence of $Cl^\bullet$ is understandable.

The probability of the recombination of $Cl^\bullet$ with a solvated electron and the stability constant for the formation of a

chlorocomplex make the oxidation of gold slower in comparison to the corresponding bromocomplex.[45] Again, disproportionation of $AuBr_2^-$ and $AuCl_2^-$ is observed from the spectroscopic investigation (appearance of a 330 nm peak via a 289 nm peak).[46]

Therefore, a plausible mechanism for the dissolution of colloidal gold may be formulated as follows. The photoirradiation of gold particles results in the formation of a chlorine radical ($Cl^\bullet$) and solvated electrons from the adsorbed Cl^- ions on the gold surface.[46] The $Cl^\bullet$ presumably, then, generates $Br^\bullet$ which oxidizes the colloidal gold.[47] The Au(I) ion thus formed combines with two Br^- to give $AuBr_2^-$, which dissolves in toluene by forming a soluble ion pair with the cetyltrimethylammonium ion. The Au(I) is then further oxidized by $Br^\bullet$ to higher valent Au(III), giving rise to $AuBr_4^-$ complexes.

$$Cl^-(ads) \rightarrow Cl^\bullet + e^-(solv)$$

$$Cl^\bullet + Br^- \rightarrow Cl^- + Br^\bullet$$

$$Au + Br^\bullet + [C_{16}TA]^+Br^- \rightarrow [C_{16}TA]^+[AuBr_2]^-$$

$$[C_{16}TA]^+[AuBr_2]^- + 2Br^\bullet \rightarrow [C_{16}TA]^+[AuBr_4]^-$$

When trivalent gold bromide, $AuBr_4^-$, is further irradiated, it forms Au(I) in successive steps. However, the Au(I) ions are neither reduced further nor do they readily disproportionate in the presence of a trace of remaining Au(III) because the redox potential of $E^\circ_{AuI/Au0}$ is quite negative,[46] and this leads to the accumulation of $AuBr_2^-$, as evidenced from the increase in intensity of the 289 nm peak (Figure 9).

Surface Functionalization of Gold Nanoparticles: An Enhanced Emission from Surface-Bound Fluorophores. In recent years, the unique physical and chemical properties of the surfaces of solid are attracting increased attention in both basic science and technology.[48,49] As the size of the particles shrinks into the nanometer regime, there is an increasingly important role of the surface in controlling the overall energy of the particles. Noble metal clusters in the nanometer size regime display widely interesting physicochemical properties that have gained increased scientific interest from the photochemists and photobiologists for organic functionalization of metal nanoparticles and exploit their role in a number of photophysical studies. Modification of gold nanoparticles with fluorophores is important for the development of biological traces as well as optoelectronic devices.[50] Pyrene and its derivatives are well-known fluorescent probes, since they possess a number of well-characterized photophysical and photochemical properties that have enabled several researchers to study their emission behavior in a variety of microenvironments.[51] Kamat et al.[52] described the organization of methylaminopyrene molecules on the tetraoctylammonium bromide-stabilized gold organosol that led to manifold fluorescent enhancement from surface-bound fluorophores. We have recently studied the emission behavior of 1-methylaminopyrene in the presence of 10 different sizes of citrate-stabilized gold nanoparticles. In that study, we observed that the probe molecules adsorbed onto the metallic surfaces suffer strong quenching of their fluorescence and the rate of quenching efficiency with particle size is different for two different size regimes of the gold particles.[53] Here, we have exploited C_{18}-TAC-stabilized gold organosol in THF to examine the emission behavior of 1-methylaminopyrene and to study the adsorbate−particle interactions in a gold−probe assembly.

The emission spectrum of MAP (1.0 μM) in THF possesses well-defined emission bands ($\lambda_{ex} \sim 328$ nm) with maxima at 377, 397, and 417 nm (Figure 10, trace a) corresponding to the monomeric form of fluorophore.[52] In the presence of surfactant-mediated gold colloids (10 μM), the emission intensity (average of seven determinations) is enhanced; SD = ±3% (Figure 10, trace b). It was noted that gold nanoparticles are nonfluorescent and also no such enhanced emission was seen when we added a THF solution of MAP containing C_{18}TAC and treated with $NaBH_4$. All the spectral measurements were done against a solvent blank. The absorption spectra of Au−C_{18}TAC (50 μM) in THF exhibit surface plasmon absorption with a maximum at 530 nm, as shown by trace a in Figure 11. When MAP is added to the gold sol, the surface plasmon band is damped (Figure 11, trace b), indicating the attachment of probe molecules to the particle surface. The gold atoms on the surface of the nanoparticles possess unoccupied orbitals for nucleophiles to donate electrons. Strong electron donors such as MAP contain an amine functionality as the end group and donate electrons to the vacant orbitals on the gold surface.[54]

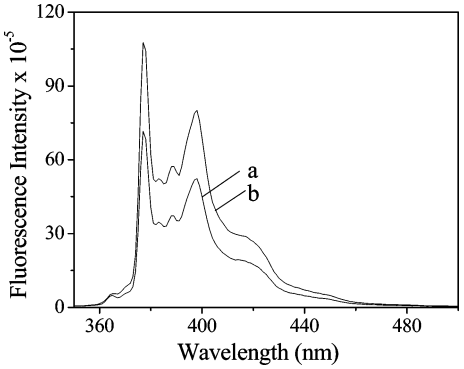

Figure 10. Emission spectra of (a) free and (b) gold-bound MAP in THF. Conditions: [MAP] = 1 μM and [Au] = 10 μM.

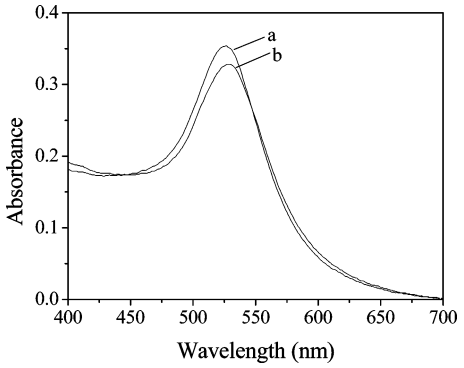

Figure 11. Absorption spectra of C_{18}TAC-stabilized gold particles (50 μM) in THF (a) before and (b) after the addition of MAP (1 μM).

The observed increase in fluorescence intensity can be elucidated by considering the proximity effects between the probe molecules and the metal particles in the nanometer length scale. It is now well established that, in a closer proximity between the nanoparticles and the probe molecule, the luminescence properties of the fluorophore are dominated by very short-ranged, near-field coupling effects.[55,56] In direct contact with the metal, the fluorescence is completely quenched.[57] The stabilizing ligand plays a role in controlling the proximity between the metal particles and the probe molecules. In our previous report, the methylaminopyrene molecules replace the citrate ions and become directly adsorbed onto the gold surface owing to complete quenching of molecular fluorescence.[53] However, in the present experiment, the longer chain surfactant molecules electrostatically bound to the gold surface render the probe molecules to donate electrons from a particular distance

to the gold surface. In such a closer proximity, the luminescence properties of the fluorophores are dominated especially by the highly localized near-field interactions,[58] leading to fluorescence enhancement of the probe molecules near the surface of metallic nanostructures. Under these circumstances, the fluorophore is excited directly and spontaneously emits; the spectral changes observed then result from the excited-state resonance interaction with the free electrons on the metallic surface. The surface functionalized gold colloids under investigation are in the subwavelength scale and that, too, without a solid support; all of these facts endorse surface plasmon coupling between the metal particles and the probe molecules.[59]

Conclusions

An organic-solution-based synthetic technique for the size-selective synthesis of gold organosol using cationic surfactants of variable chain lengths has been reported. Gold nanoparticles stabilized by C_nTAC ($n = 10-18$) possess well-defined surface plasmon absorption, and its formation can be investigated by following the changes in the absorption profile during the reduction process. The synthetic technique is very simple, and the metal nanoparticles prepared by this method exhibit excellent solubility in a wide range of nonpolar organic solvents. The tendency of the gold particles to coalesce in organic solvents with the decreased chain length of surfactants has been rationalized from the decrease in particle−particle interaction energies. We have focused on the stability of gold particles in a variety of environments and elucidated the stabilization phenomenon on the basis of several physical and chemical aspects of colloid chemistry. The role of the counterion of the phase transfer reagent and stabilizing ligand shell on the photochemical stability of gold colloids has been investigated. We have succeeded in achieving organization of pyrene chromophores around gold nanoparticles, through surface binding of the amine moiety, and have found an enhancement of methylaminopyrene fluorescence in the vicinity of nanostructured gold particles.

Acknowledgment. The authors are thankful to UGC and CSIR, New Delhi, for financial assistance.

References and Notes

(1) (a) Belloni, J.; Amblad, J.; Marignier, J. L.; Mostafavi, M. In *Clusters of Atoms and Molecules*; Haerland, H., Ed.; Springer-Verlag: Berlin, 1994; Vol. II, pp 290−311. (b) Pipino, A. C. R.; Schatz, G. C.; Van Duyne, R. P. *Phys. Rev. B* **1996**, *53*, 4162. (c) Henglein, A. *Chem. Rev.* **1989**, *89*, 1861. (d) Belloni, J.; Mostafavi, M.; Remita, H.; Marignier, J. L.; Delcourt, M. O. *New J. Chem.* **1998**, *22*, 1239.

(2) (a) Belloni, J. *Curr. Opin. Colloid Interface Sci.* **1996**, *1*, 184. (b) Elghanian, R.; Storhoff, J. J.; Mucic, R. C.; Letsinger, R. L.; Mirkin, C. A. *Science* **1997**, *277*, 1078.

(3) Lieber, C. M. *Solid State Commun.* **1998**, *107*, 607.

(4) (a) Sau, T. K.; Pal, A.; Pal, T. *J. Phys. Chem. B* **2001**, *105*, 9266. (b) Narayanan, R.; El-Sayed, M. A. *Nano Lett.* **2004**, *4*, 1343.

(5) (a) Klein, D. L.; McEuen, P. L.; Katari, J. E.; Roth, R.; Alivisatos, A. P. *Appl. Phys. Lett.* **1996**, *68*, 2574. (b) Dulkeith, E.; Morteani, A. C.; Niedereichholz, T.; Klar, T. A.; Feldmann, J.; Levi, S. A.; van Veggel, F. C. J. M.; Reinhoudt, D. N.; Möller, M.; Gittins, D. I. *Phys. Rev. Lett.* **2002**, *89*, 203002-1.

(6) (a) Henglein, A. *J. Phys. Chem.* **1993**, *97*, 5457. (b) Henglein, A. *Ber. Bunsen-Ges. Phys. Chem.* **1995**, *99*, 903.

(7) Schmid, G. *Clusters and Colloids—From Theory to Applications*; VCH: Weinheim, Germany, 1994.

(8) Kreibig, U.; Vollmer, M. *Optical Properties of Metal Clusters*; Springer: Berlin, 1995.

(9) Link, S.; El-Sayed, M. A. *Int. Rev. Phys. Chem.* **2000**, *19*, 409.

(10) Templeton, A. C.; Pietron, J. J.; Murray, R. W.; Mulvaney, P. *J. Phys. Chem. B* **2000**, *104*, 564.

(11) Malinsky, M. D.; Kelly, K. L.; Schatz, G. C.; Van Duyne, R. P. *J. Am. Chem. Soc.* **2001**, *123*, 1471.

(12) Ghosh, S. K.; Nath, S.; Kundu, S.; Esumi. K.; Pal, T. *J. Phys. Chem. B* **2004**, *108*, 13963.

(13) Avouris, P.; Persson, B. N. J. *J. Phys. Chem.* **1984**, *88*, 837.

(14) Ipe, B. I.; George Thomas, K.; Barazzouk, S.; Hotchandani, S.; Kamat, P. V. *J. Phys. Chem. B* **2002**, *106*, 18.

(15) Hranisavljevic, J.; Dimitrijevic, N. M.; Wurtz, G. A.; Wiederrecht, G. P. *J. Am. Chem. Soc.* **2002**, *124*, 4536.

(16) Prasad, B. L. V.; Stoeva, S. I.; Sorensen, C. M.; Klabunde, K. J. *Langmuir* **2002**, *18*, 7515.

(17) Zhang, J.; Whitesell, J. K.; Fox, M. A. *J. Phys. Chem. B* **2003**, *107*, 6051.

(18) Bhattacharya, S.; Srivastava, A. *Langmuir* **2003**, *19*, 4439.

(19) Roy Mason, W., III; Gray, H. B. *Inorg. Chem.* **1968**, *7*, 55.

(20) Vogel, A. I. *A Text Book of Quantitative Inorganic Analysis*, 4th ed.; Longman: London, 1978.

(21) Link, S.; El-Sayed, M. A. *J. Phys. Chem. B* **1999**, *103*, 8410.

(22) Pal, A.; Ghosh, S. K.; Esumi, K.; Pal, T. *Langmuir* **2004**, *20*, 575.

(23) Mafuné, F.; Kohno, J.; Takeda, Y.; Kondow, T.; Sawabe, H. *J. Phys. Chem. B* **2000**, *104*, 8333.

(24) Mafuné, F.; Kohno, J.; Takeda, Y.; Kondow, T.; Sawabe, H. *J. Phys. Chem. B* **2000**, *104*, 9111.

(25) Jin, R.; Cao, Y. W.; Mirkin, C. A.; Kelly, K. L.; Schatz, G. C.; Zheng, J. G. *Science* **2001**, *294*, 1901.

(26) Huang, Z. Y.; Mills, G.; Hajek, B. *J. Phys. Chem.* **1993**, *97*, 11542.

(27) Ghosh, S. K.; Kundu, S.; Mandal, M.; Nath, S.; Pal, T. *J. Nanopart. Res.* **2003**, *5*, 577.

(28) Mafuné, F.; Kohno, J.; Takeda, Y.; Kondow, T. *J. Phys. Chem. B* **2001**, *105*, 5114.

(29) Esumi, K.; Azusa, K.; Suzuki, A.; Torigoe, K. *Colloids Surf., A* **2001**, *189*, 155.

(30) Templeton, A. C.; Pietron, J. J.; Murray, R. W.; Mulvaney, P. *J. Phys. Chem. B* **2000**, *104*, 564.

(31) Ohara, P. C.; Leff. D. V.; Heath, J. R.; Gelbart, W. M. *Phys. Rev. Lett.* **1995**, *75*, 3466.

(32) Nikoobakht, K.; El-Sayed, M. A. *Langmuir* **2001**, *17*, 6368.

(33) Manna, L.; Scher, E. C.; Alivisatos, A. P. *J. Am. Chem. Soc.* **2000**, *122*, 12700.

(34) Mulvaney, P.; Liz-Marzan, L. M.; Giersig, M.; Ung, T. *J. Mater. Chem.* **2000**, *10*, 1259.

(35) Hiemenz, P. *Principles of Colloids and Surface Chemistry*; Marcel Dekker: New York, 1986.

(36) Kreibig, U.; Genzel, L. *Surf. Sci.* **1985**, *156*, 678.

(37) Su, K.-H.; Wei, Q.-H.; Zhang, X.; Mock, J. J.; Smith, D. R.; Schultz, S. *Nano Lett.* **2003**, *3*, 1087.

(38) Pengo, P.; Pasquato, L.; Scrimin, P. *J. Supramol. Chem.* **2002**, *2*, 305.

(39) Hunter, R. J. *Foundations of Colloid Science*; Oxford University Press: New York, 1989; Vol. 1.

(40) Israelachvili, J. *Intermolecular and Surface Forces*, 2nd ed.; Academic Press: San Diego, CA, 1992.

(41) Sastry, M. *Curr. Sci.* **2004**, *85*, 1735.

(42) George Thomas, K.; Zajicek, J.; Kamat, P. V. *Langmuir* **2002**, *18*, 3722.

(43) Pal, T.; Sau, T. K.; Jana, N. R. *Langmuir* **1997**, *13*, 1481.

(44) Malone, K.; Weaver, S.; Taylor, D.; Cheng, H.; Sarathy, K. P.; Mills, G. *J. Phys. Chem. B* **2002**, *106*, 7422.

(45) Cotton, F. A.; Wilkinson, G. *Advanced Inorganic Chemistry*, 5th ed.; Wiley-Interscience: Singapore, 1988; p 948.

(46) Gachard, E.; Remita, H.; Khatouri, J.; Keita, B.; Nadjo, L.; Belloni, J. *New J. Chem.* **1998**, *22*, 1257.

(47) Nakao, Y. *J. Chem. Soc., Chem. Commun.* **1994**, 2067.

(48) Avouris, P.; Persson, B. N. J. *J. Phys. Chem.* **1984**, *88*, 837.

(49) Alivisatos, A. P. *Science* **1996**, *271*, 933.

(50) Hickman, J. J.; Ofer, D.; Laibnis, P. E.; Whitesides, G. M.; Wrighton, M. S. *Science* **1991**, *252*, 688.

(51) (a) Förster, T.; Selinger, B. K. *Z. Naturforsch.* **1964**, *A19*, 38. (b) Kalyanasundaram, K.; Thomas, J. K. *J. Am. Chem. Soc.* **1977**, *99*, 2039. (c) Bertolotti, S. G.; Zimmerman, O. E.; Cosa, J. J.; Previtali, C. M. *J. Lumin.* **1993**, *55*, 105. (d) Ghosh, S. K.; Pal, A.; Kundu, S.; Mandal, M.; Nath, S.; Pal, T. *Langmuir* **2004**, *20*, 5209.

(52) George Thomas, K.; Kamat, P. V. *J. Am. Chem. Soc.* **2000**, *122*, 2655.

(53) Ghosh, S. K.; Pal, A.; Kundu, S.; Nath, S.; Pal, T. *Chem. Phys. Lett.* **2004**, *395*, 366.

(54) Makarova, O. V.; Ostafin, A. E.; Miyoshi, H.; Norris, J. R., Jr., Miesel, D. *J. Phys. Chem. B* **1999**, *103*, 9080.

(55) Chance, R. R.; Prock, A.; Silbey, R. *Adv. Chem. Phys.* **1978**, *37*, 1.

(56) Whitmore, P. M.; Robota, H. J.; Harris, C. B. *J. Chem. Phys.* **1982**, *76*, 740.

(57) Ditlbacher, H.; Krenn, J. R.; Felidj, N.; Lamprecht, B.; Schider, G.; Salerno, M.; Leitner, A.; Aussenegg, F. R. *Appl. Phys. Lett.* **2002**, *80*, 404.

(58) Hamann, H. F.; Kuno, M.; Gallagher, A.; Nesbitt, D. J. *J. Chem. Phys.* **2001**, *114*, 8598.

(59) (a) Aslan, K.; Gryczynski, I.; Malicka, J.; Matveeva, E.; Lakowicz, J. R.; Geddes, C. D. *Curr. Opin. Biotechnol.* **2005**, *16*, 55. (b) Drexhage, K. H. In *Progress in Optics XII*; Wolf, E., Ed.; North-Holland: Amsterdam, The Netherlands, 1974; p 165. (c) Larkin, I. A.; Stockman, M. I.; Achermann, M.; Klimov, V. I. *Phy. Rev. B* **2004**, *69*, 121403.